The Structure of the N-Terminus of Striated Muscle α-Tropomyosin in a Chimeric Peptide: Nuclear Magnetic Resonance Structure and Circular Dichroism Studies[†,‡]

Norma J. Greenfield,*[,§] Gaetano T. Montelione,[||] Ramy S. Farid,[⊥] and Sarah E. Hitchcock-DeGregori[§]

Department of Neuroscience and Cell Biology, Robert Wood Johnson Medical School, University of Medicine and Dentistry of New Jersey, 675 Hoes Lane, Piscataway, New Jersey 08854-5635, Center for Advanced Biotechnology and Medicine, 679 Hoes Lane, Piscataway, New Jersey 08954-5639, and Department of Chemistry, Rutgers University, 73 Warren St., Newark, New Jersey 07102

Received December 29, 1997; Revised Manuscript Received March 24, 1998

ABSTRACT: Tropomyosins (TMs) are highly conserved, coiled-coil, actin binding regulatory proteins found in most eukaryotic cells. The amino-terminal domain of 284-residue TMs is among the most conserved and functionally important regions. The first nine residues are proposed to bind to the carboxyl-terminal nine residues to form the "overlap" region between successive TMs, which bind along the actin filament. Here, the structure of the N-terminus of muscle α-TM, in a chimeric peptide, TMZip, has been solved using circular dichroism (CD) and two-dimensional proton nuclear magnetic resonance (2D ^{1}H NMR) spectroscopy. Residues 1−14 of TMZip are the first 14 N-terminal residues of rabbit striated α-TM, and residues 15−32 of TMZip are the last 18 C-terminal residues of the yeast GCN4 transcription factor. CD measurements show that TMZip forms a two-stranded coiled-coil α-helix with an enthalpy of folding of −34 ± 2 kcal/mol. In 2D^{1}H NMR studies at 15 °C, pH 6.4, the peptide exhibits 123 sequential and medium range intrachain NOE cross peaks per chain, characteristic of α-helices extending from residue 1 to residue 29, together with 85 long-range NOE cross peaks arising from interchain interactions. The three-dimensional structure of TMZip has been determined using these data plus an additional 509 intrachain constraints per chain. The coiled-coil domain extends to the N-terminus. Amide hydrogen exchange studies, however, suggest that the TM region is less stable than the GCN4 region. The work reported here is the first atomic-resolution structure of any region of TM and it allows insight into the mechanism of the function of the highly conserved N-terminal domain.

Tropomyosins (TMs)[1] form a highly conserved family of actin binding proteins found in most eukaryotic cells (*1*). Tropomyosin binds to actin cooperatively and also cooperatively regulates the thin filament's interaction with myosin. Together with troponin in striated muscles, TM makes the regulation Ca^{2+}-sensitive (*2, 3*). Both the N- and C-terminal regions of TM are critical for normal function (*4, 5*).

Tropomyosin is a two-stranded α-helical coiled coil, and the chains are arranged in parallel and in register (*6*−*8*). The 9-Å structure of striated α-TM shows it to be coiled-coil over most of its length, but the structure of the overlap region, comprised of the first and last nine amino acids, is poorly resolved (*9, 10*). It has been suggested that the four chains of the overlap region form a compact globular domain (*9*), though the original analysis of the sequence included them in the coiled coil (*6*). Tropomyosin is associated head-to-tail, via the overlap regions, in the long pitch grooves of the helical actin filaments (*11, 12*).

The N-terminal region of TM is highly conserved in the 284-residue TMs found in muscle and nonmuscle cells, being identical in *Drosophila* and rabbit (*1, 13*). Its integrity is critical for the function of striated TM. Removal of the *N*-acetyl group from the N-terminal Met of striated α-TM results in a major reduction of actin affinity, loss of polymerizability (as measured using high shear viscosity), and altered cooperative regulation of the acto-myosin S1 ATPase (*14*−*17*). Removal of the first 10 residues results in loss of actin affinity, even in the presence of troponin (*18*). Individuals carrying a mutation of the residue corresponding to Met-8 to Arg in a closely related tropomyosin, TPM3, exhibit nemaline myopathy, a disease of striated muscle (*19*). Introduction of a Met8Arg mutation into recombinant striated α-TM results in a major reduction in actin affinity (Hitchcock-DeGregori and Liu, unpublished results).

To gain insight into the function of the N-terminus of tropomyosin we have determined its structure in a model peptide using high-resolution two-dimensional NMR spectroscopy. The thermodynamics of folding and hydrogen-exchange properties of the peptide were also examined. The peptide, called TMZip, contains 32 amino acids: residues 1−14 correspond to residues 1−14 of striated rabbit α-TM (*20, 21*), while residues 15−32 correspond to the C-terminal 18 residues (264−281) of the yeast GCN4 transcription factor (*22*). In this model peptide, the highly conserved N-terminal

[†] This work was supported by NIH Grant RO1 GM36326 and shared instrumentation Grant RR 10425 from the NIH.

[‡] Coordinates for the 15 structures of TMZip and the associated restraint files have been deposited at the Brookhaven Protein Data Bank under the file name 1TMZ. NMR data have been deposited at BioMagResBank under accession number 4133.

[§] Robert Wood Johnson Medical School.

[||] Center for Advanced Biotechnology and Medicine.

[⊥] Department of Chemistry, Rutgers University.

[1] Abbreviations: NOE, nuclear overhauser effect; TM, tropomyosin.

S0006-2960(97)03167-X CCC: $15.00
Published on Web 05/08/1998

Table 1: Sequence of the TMZip Peptide Compared to α-Tropomyosin[a]

Residue	1				5				10					15					20					25					30			
α-Tropomyosin	M	D	A	I	K	K	K		M	Q	M	L	K	L	D	K	E	N	A	L	D	R	A	E	Q	A	E	A	D	K	K	A	A
TMZip	M	D	A	I	K	K	K		M	Q	M	L	K	L	D	N	Y	H	L	E	N	E	V	A	R	L	K	K	L	V	G	E	R
Heptad Position	*a*			*d*					*a*			*d*				*a*			*d*					*a*			*d*				*a*			*d*

[a] The sequences of rabbit α-tropomyosin (residues 1−32) and TMZip (residues 1−14) are from Stone and Smillee (*21*) and the sequence of residues 15−32 of TMZip corresponds to that of the last 18 C-terminal residues (264−281) of the yeast transcription factor GCN4 (Landschultz et al., *22*).

domain of α-TM was kept intact, while a short stable coiled-coil region of the "leucine zipper" domain of GCN4 (*22*) was used to replace the long coiled-coil domain of the rest of the α-TM molecule. The results show that TMZip is an α-helical coiled coil from residues 1−29, but that the coiled coil of the TM region is less stable than the GCN4 region. The work reported here is the first atomic-resolution structure of any region of TM.

MATERIALS AND METHODS

Peptide Synthesis. TMZip (Table 1) was synthesized by SynPep (Dublin, CA). The peptide was greater than 95% pure when analyzed by reverse-phase HPLC on a C-18, 5 μ, 40 × 100 mm column. The molecular weight, determined by electrospray mass spectroscopy (SynPep), 3885.0, was within the limits of accuracy of the technique of the weight of 3885.7 expected from the amino acid sequence. The mass spectrum also indicated that the sample was greater than 95% homogeneous.

Circular Dichroism Measurements. CD measurements were made using an Aviv model 62 DS spectropolarimeter as previously described (*23*). The protein concentrations of peptide stock solutions (two peptide chains per molecule) were determined from measurements of their difference spectra in 6M guanidine-HCl between pH 12.5 and pH 6.0 using an extinction coefficient of 4714 M^{-1} cm^{-1} at 294 nm (*24*−*26*).

Determination of the Enthalpy of Folding. The enthalpy and T_M of folding of TMZip were estimated from changes in the CD spectra as a function of temperature using the following equations:

$$k = \exp\{(\Delta H/RT)((T/T_{Mobs}) - 1) - \ln [C]\} \quad (1)$$

$$y = \{(4[C]k + 1) - (8[C]k + 1)^{(1/2)}\}/4[C]k \quad (2)$$

$$\theta_{obs} = (\theta_{max} - \theta_{min})y + \theta_{min} \quad (3)$$

where θ_{obs} is the ellipticity found at any temperature, θ_{max} is the maximum ellipticity corresponding to the fully folded peptide, θ_{min} is the ellipticity corresponding to the unfolded peptide, [C] is the molar peptide concentration, ΔH is the van't Hoff enthalpy of folding, T is the absolute temperature, T_{Mobs} is the midpoint of the folding transition observed at each peptide concentration, and R is the gas constant. θ_{max}, θ_{min}, T_{Mobs}, and ΔH were all estimated by nonlinear least squares curve fitting using the commercial program SigmaPlot 5.0 (Jandel Scientific). The T_M of the transition was determined by determining ΔG and ΔS at T_{Mobs} using the relationships $\Delta G = -nRT\ln K$ and $\Delta G = \Delta H - T\Delta S$ and then determining the T_M at $\Delta G = 0$, ($K = 1$) where $T_M = \Delta H/\Delta S$. This treatment assumes that the change in heat capacity (ΔC_p) is negligible during unfolding. The values of ΔH, T_M, and ΔC_p were also estimated from the change in CD using equations which included the ΔC_p terms (*27*, *28*).

Deconvolution of Circular Dichroism Spectra. CD spectra were deconvoluted into component curves by the convex constraint analysis program of Perczel et al. (*29*, *30*) as previously described (*23*).

NMR Measurements. For structural assignments, two-dimensional proton NMR measurements of the TMZip peptide, 1 mM (two-chained species, molecular mass = 7772 Da), in 10 mM sodium phosphate, 100 mM NaCl, pH 6.4 in 95% ^1H_2O, 5% ^2H_2O were made on a Varian Unity 500-MHz NMR spectrometer (Varian Associates, Palo Alto, CA) at 15 °C. The following spectra were accumulated: 2QF-COSY (*31*) and NOESY (*32*), with mixing times of 50, 150, and 300 ms, and TOCSY (*33*), with mixing times of 15, 45, 60, 80, and 100 ms. For all spectra, the sweep width was 6000 Hz in both $\omega 1$ and $\omega 2$ and 32−64 transients were collected for each increment. The TOCSY and 2QF-COSY spectra were collected using the TPPI method of quadrature detection in $\omega 2$ (*34*) while the NOESY spectra were collected using the hypercomplex method (*35*). For the TOCSY and NOESY spectra, 4096 complex points were collected in $\omega 2$ and 512−800 complex points were collected in $\omega 1$. Spectra were zero filled to 2048 complex points in $\omega 1$. For the 2QF-COSY spectrum, 4096 complex points were collected in $\omega 2$ and 1024 in $\omega 1$. Spectra were zero filled to 2048 points in $\omega 1$. All the NOESY and TOCSY spectra were processed with VNMR (Varian Associates, Palo Alto, CA) with negative line broadenings of −2 Hz and Gaussian multiplications in $\omega 2$, and negative line broadening of −10 to −30 Hz and Gaussian or sine-bell multiplication in $\omega 1$. Spectra were processed with first point multiplication in $\omega 2$ and were corrected for baseline drift in both dimensions. $^3J(H^N\text{-}H^\alpha)$ coupling constants were estimated from the distances between the positive and negative H^N-H^α cross peaks in the 2QF-COSY spectrum.

Sequence-Specific Assignments and Secondary Structure. Resonance assignments were determined by standard homonuclear NMR methods (*36*). The 2QF-COSY and TOCSY spectra were used to identify the spin systems of the amino acid residues of TMZip. The NOESY spectra with mixing times of 150 and 300 ms were then used to determine the H^N_i-H^N_{i+1}, H^α_i-H^N_{i+1}, and H^β_i-H^N_{i+1} NOE cross peaks and to establish the sequence-specific resonance assignments. Residues involved in α-helical conformations were identified on the basis of their characteristic short-range NOE cross peaks (*36*).

Tertiary Structure Determination. Interatomic distances of the protons in TMZip were quantified using a NOESY spectrum recorded with a mixing time of 50 ms. The relative volumes of the peaks were determined using the peak

peaking routine (ll2d) available in the VNMR software package. The NOESY cross peak volumes were interpreted in terms of internuclear distances using a simple two-spin approximation, calibrated using well-resolved $\beta\beta$ and $\gamma\gamma$ cross peaks in the spectrum, which correspond to a fixed interatomic distance of 1.77 Å. The resulting distance estimates were then converted into upper-bound distance constraints by rounding to the next highest 0.5 Å. Pseudoatom corrections (*37*) were made for those peaks whose stereospecific assignments were unknown and for methylene, methyl, and isopropyl methyl protons whose chemical shifts were degenerate.

Calculations of the tertiary structure of TMZip were performed using the program DIANA (*38, 39*). The resonances associated with the methyl groups of the N-terminal acetyls were not assigned and these acetyl groups were not included in the calculations of the structures. To perform the structure calculations, the two chains were linked together by an artificial flexible linker containing only pseudoatoms. A total of 127 intraresidue, 191 sequential, 314 medium range [$1 < (I - j) \leq 5$] range intrachain, and 85 long range [$(I - j) > 5$] interchain NOE cross peaks per chain were included in the calculations. Dihedral angle constraints consistent with α-helical structures ($\phi = -57 \pm 20$, $\psi = -47 \pm 20$) were imposed on 6 residues/chain, where the patterns of short-range NOE cross peaks were indicative of α-helical structure and the $^3J(H^N\text{-}H^\alpha)$ coupling constants were < 5 Hz. Two hundred random structures were used as starting points, and a 33-step minimization procedure was used in the DIANA calculations. The minimization was then repeated using as starting points the 100 conformers that gave the lowest constraint violations in the first minimization. No explicit hydrogen bond constraints were used in the DIANA calculations.

Structural Analysis. The program MolMol (*40*) was used to superimpose the 15 best set of conformers from the DIANA calculations. The heavy atoms were aligned and the average values and root-mean-square distances (rmsds) were calculated using the program. In addition, MolMol was used to identify the hydrogen bonds in the structures. The percentage of each residue exposed to the solvent in the average NMR structure of TMZip was also calculated using the MolMol program (*40*).

Hydrogen Exchange. Hydrogen exchange experiments of TMZip were performed by dissolving a lyophylized sample of peptide containing NaCl and sodium phosphate in ^2H_2O at 4 °C to a final concentration of 1 mM peptide, 100 mM NaCl, 10 mM phosphate, pH 5.8 (uncorrected). The freshly dissolved sample was immediately transferred to an NMR tube and placed in the NMR probe, pre-equilibrated at 12.5 °C, and collection of the NOESY spectra, with mixing times of 50 ms, was started within five minutes. Fourteen consecutive NOESY spectra were collected with sweep widths of 6000 Hz in both dimensions and 4096 complex points collected in $\omega 2$ and 96 complex points in $\omega 1$. Eight transients were averaged at each increment and each 2D data set took approximately 20 min to collect. Data were processed with linear prediction in the $\omega 1$ dimension and zero filling to 512 complex points. The volumes of the peaks arising from the slowly exchanging amides in each 2D spectrum were normalized to the C2 and C4 protons of the single histidine residue/chain. The relative rates of exchange of well-resolved NH protons were quantified by following the rate of disappearance of their diagonal peaks in the NOESY spectra, since these had much higher signal-to-noise than the cross peaks. Two of the diagonal H^N peaks, however, arising from Ala-23 and Val-29 overlapped. The rates of exchange of these protons were resolved by following the loss of the cross peaks to the αH, βH, and β and γ methyl protons respectively as a function of time. The protection factor from exchange was defined as the observed rate divided by the rate expected if TMZip was in a random coil conformation. The expected random coil rates were calculated as described by Bai et al. (*41*), which takes into account the effects of neighboring side chains on the neutral, base-, and acid-catalyzed rates of exchange of the NH protons of each amino acid in a given sequence at a given pH (corrected for the effect of deuterium oxide on the reading from the pH meter).

Homology Modeling. Prior to the determination of the tertiary structure of TMZip from the NMR NOE data, its conformation was modeled based on its homology to the leucine zipper GCN4-P1 peptide (*42*), which consists of the 33 C-terminal residues of GCN4, using the program Sybyl (Tripos Associates). The coordinates of the GCN4 peptide were from the Brookhaven Protein Data Bank, file 2ZTA. The N-terminal amino acid of the GCN4-P1 peptide (Arg-1) was deleted and the side chains of residues 2−15, starting at Met-2 (an *a* position in the heptapeptide repeat of coiled coils), were replaced with the side chains of the first 14 residues of rabbit striated muscle α-tropomyosin (*20, 21*). The acidic and basic side chains were all assumed to be charged at neutral pH. Minimization was performed using the Kollman all-atom force field with Kollman charges, a distance-dependent dielectric constant of 1.0, and a nonbonding cutoff of 9.5 Å. The conjugate-gradient minimizations were performed until the energy gradient (rms force) reached 0.001 kcal mol^{-1} $Å^{-1}$. The native GCN4 structure was first minimized to yield a structure with only 0.16 Å rmsd (of all nonhydrogen backbone atoms) from the original X-ray structure, demonstrating that the force field used did not significantly perturb the original structure. TMZip was then minimized using the same conditions. The final minimized structure had a backbone rmsd of 0.15 Å from the minimized GCN4 structure.

RESULTS

Peptide Design. The goal of the present study was to determine the structure of the highly conserved N-terminus of tropomyosin. We used a chimeric peptide, TMZip, in which residues 1−14 are the first 14 residues of the N-terminus of rabbit striated α-tropomyosin (*20, 21*) and residues 15−32 are the last 18 C-terminal residues of the 33-residue GCN4-P1 peptide (*43*), a short stable coiled-coil α-helix, and the leucine zipper region (residues 249−281) of the yeast GCN4 DNA transcription factor (*22, 43*). The sequence of TMZip, compared to the first 32 residues of rabbit α-TM (*21*) is given in Table 1. Chimeras such as TMZip have been successfully used to study the functions of DNA transcription factors (*44*) and smooth muscle myosin (*45*). Short segments of the GCN4 leucine zipper have been substituted for segments of striated muscle α-TM without major loss of actin binding affinity or regulatory function (*46, 47*).

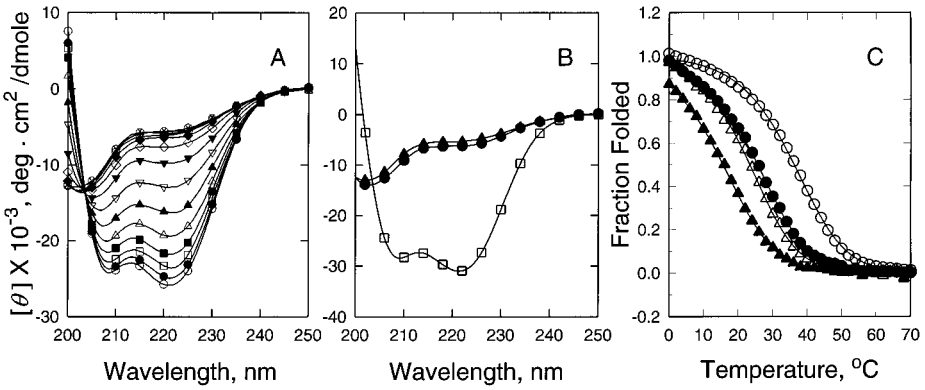

FIGURE 1: (A) The change in the circular dichroism spectrum of TMZip at a concentration of 15 μM as a function of temperature (○, 0; ●, 5; □, 10; ■, 15; △, 20; ▲, 25; ▽, 30; ▼, 35; ◇, 40; ◆, 45; ×, 50; +, 55; ⊗, 60 °C). (B) The data in 2A deconvoluted into three curves using the convex constraint algorithm (*29*). (C) The change in the fraction folded, determined from changes in the CD at 222 nm as a function of temperature, at four concentrations of TMZip, 1.5, 7.5, 15, and 150 μM. The points are the raw data, and the lines are the best fits, assuming that the peptide dissociates in a two-state cooperative transition between a folded dimer and an unfolded monomer. For clarity, only every tenth raw data point is illustrated.

Table 2: Thermodynamic Parameters of Folding of the TMZip Peptide

conc (μM)	ΔH (kcal/mol)	$T_{M(observed)}$ (°C)	ΔS (cal/mol deg)	$T_{M(\Delta G=0)}$ (°C)
150	−36.4	36.2	−101.6	85.0
15	−34.3	25.6	−94.2	91.0
7.5	−36.1	23.3	−99.7	88.7
1.5	−31.7	15.6	−84.5	101.6
average	−34.6 ± 2.2		−95.0 ± 7.6	91.6 ± 7.2

Folding of TMZip. The temperature and concentration dependence (Figure 1) of the unfolding of TMZip at thermal equilibrium, followed using CD spectroscopy, was consistent with a model where a two-chained coiled-coil α-helix dissociates in a single cooperative transition to yield two single-stranded unfolded chains. There was no evidence for the formation of species with a higher number of chains. First, the data obtained as a function of temperature showed only one folding transition. Second, deconvolution of spectra obtained as a function of temperature (Figure 1A) into three curves using the convex constraint algorithm (*29, 30*) showed that the data could be fit by only two basis curves (Figure 1B). There was no evidence for a folding intermediate. Third, when the concentration and temperature dependence of the CD at 222 nm (Figure 1C) was used to estimate the thermodynamic parameters, assuming that $\Delta C_p = 0$, the analyses were only consistent with an unfolded monomer-folded dimer equilibrium. As shown in Table 2, when the T_M of the transition was evaluated at $K = 1$ where $\Delta G = 0$, there was no concentration dependence over a range of 1.5 to 150 μM, excluding the formations of species with a greater number of chains than two contributing to the change in circular dichroism. The T_M (at $\Delta G = 0$) was equal to 91.6 ± 7.2 °C, similar to that determined for the GCN4 P1 peptide (*48*). The average enthalpy of folding, assuming a monomer−dimer equilibrium, was −34.6 ± 2.2 kcal/mol, also similar to that of the GCN4-P1 peptide (*48*). Formation of a species with more than two chains is unlikely but cannot be ruled out by the CD measurements, but if such association occurs, it is not accompanied by a change in CD. Fitting the curves by equations that include terms for changes in heat capacity (*27, 28*) did not appreciably change the calculated thermodynamic parameters.

Sequential Assignments and Secondary Structure of TMZip. TMZip gave well-resolved NMR spectra in phosphate buffered saline, with a near physiological ionic strength of 0.11. Figure 2 shows the H^N-H^α cross peaks in the fingerprint region of the 2QF-COSY spectrum. Only a single set of 32 cross peaks was found, demonstrating that the folded peptide is a parallel, in register, two-chain coiled coil, as are the parent molecules, tropomyosin and the GCN4 leucine zipper.

Figure 3 shows the displacements, relative to the statistical coil, of the H^N and H^α chemical shifts of residues 1−32 of TMZip and those of homologous residues of the GCN4 P1 peptide (residues 2−33) (*43*) and the Jun LZ homodimer (residues 8−39) (*49*). The chemical shift displacements of the H^α protons arising from the α-TM portion of TMZip, residues 1−14, were similar to those of the aligned residues of the Jun LZ homodimer peptide (*49*) and two different peptides derived from GCN4, P1 (*43*) and BR-LZ (*50*). These chemical shifts were displaced upfield, consistent with the residues being in an α-helical conformation (*51*).

The sequences of coiled coils show a characteristic periodicity with a heptad repeat. When residues are labeled *a, b, c, d, e, f,* and *g*, respectively, residues in *a* and *d* positions are usually hydrophobic, and the other residues are usually hydrophilic. The displacements of the H^N chemical shifts of the N-terminus of TMZip (Figure 3) had the periodicity reported for coiled-coil peptides including GCN4 (*52*) and Jun LZ (*49*), in that the chemical shifts of the residues in *a* and *e* positions of the heptad repeat were displaced downfield, while those of the *c* and *f* positions were displaced upfield relative to those of the statistical coil. Goodman and Kim (*52*) and Junius et al. (*49*) suggested that the periodicity in the H^N chemical shifts could be a consequence of differences in hydrogen bond lengths at different positions in the heptapeptide repeat of coiled coils.

The chemical shift displacements of both the H^α and H^N protons of residues 15−32 in TMZip, arising from the GCN4 sequence in the peptide, also shown in Figure 3, were, not surprisingly, almost identical to those reported for the residues with the same sequence of the parent GCN4-P1 (*43*) and GCN4 BR-LZ (*50*) peptides, indicating that they have very similar conformations.

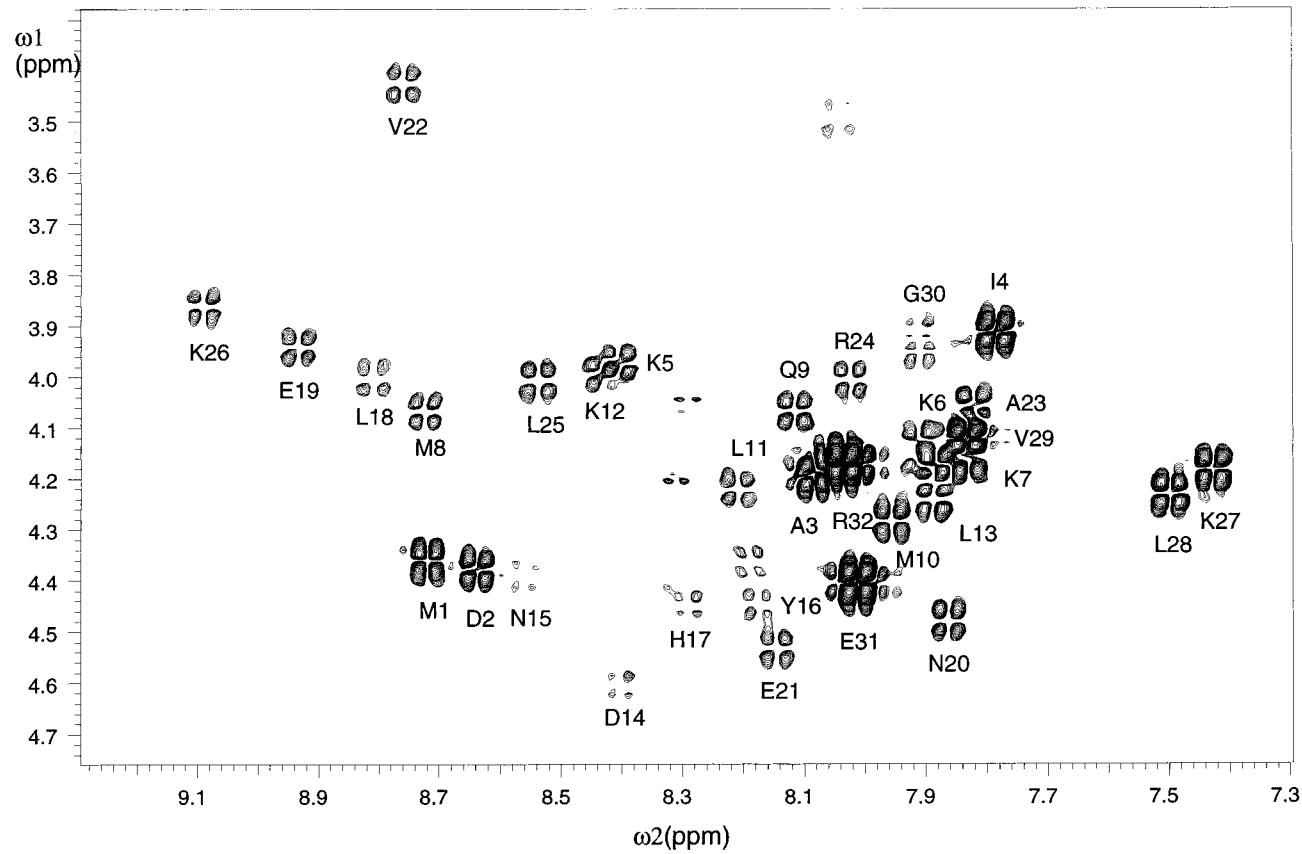

FIGURE 2: The H^{α}-H^{N} cross peaks in the fingerprint region of the 2QF-COSY spectrum of TMZip.

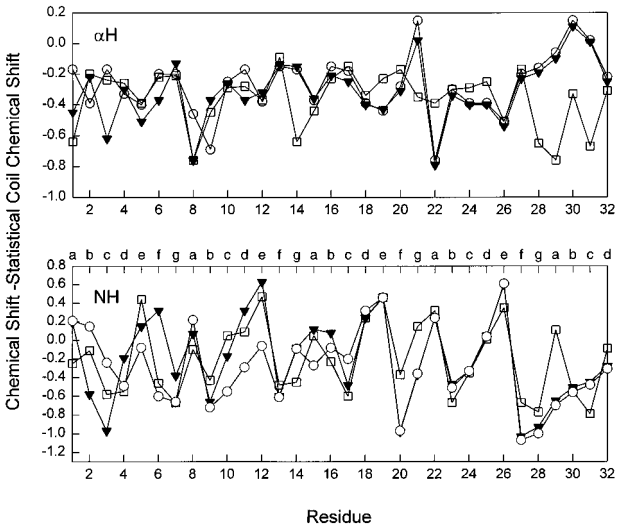

FIGURE 3: The displacements the chemical shifts, compared to those of the statistical coil of their respective sequences (36), of the αH (top) and NH (bottom) protons of each residue of TMZip (○), the GCN4 P1 peptide (▼) and the Jun LZ homodimer (□).

Figure 4 shows the H^{N}-H^{N} backbone region of the 150 ms NOESY spectrum. For clarity only the highest contour levels are displayed. The cross peaks of one set of connected resonances are labeled. Clearly resolved H^{N}_{i}-H^{N}_{i+1} NOE cross peaks were apparent for residues 1−29. When the contour threshold was lowered, many H^{N}_{i}-H^{N}_{i+2} and some H^{N}_{i}-H^{N}_{i+3} cross peaks were also observable. In addition to these cross peaks, the peptide showed H^{α}_{i}-H^{N}_{i+3}, H^{α}_{i}-H^{N}_{i+4}, and H^{α}_{i}-H^{β}_{i+3} NOE cross peaks characteristic of α-helices from residue 1 to residue 29. These findings suggest that TMZip is α-helical along its length except for the three C-terminal residues, Gly, Glu, and Arg, which are disordered in the GCN4-P1 peptide part of the molecule (*42*, *43*). The major NOE cross peaks used to determine the sequential assignments and secondary structure of TMZip are shown in Figure 5. The residues displaying $^{3}J(H^{N}$-$H^{\alpha})$ coupling constants less than 5 Hz, characteristic of α-helices, are denoted by stars. The assignments of the observed chemical shifts are summarized in the Supporting Information.

Tertiary Structure of TMZip. Since TMZip has two identical, parallel polypeptide chains, it was necessary to assign each NOE cross peak as arising from either an interchain or an intrachain interaction. To discriminate between the assignments, which are inherently ambiguous, TMZip was initially homology modeled on the structure of the GCN4 leucine zipper peptide (*42*) and the distances between each pair of protons in the model were calculated. The observed NOE cross peaks were examined individually, and they were initially assigned as either intrachain or interchain on the basis of the expected relative distances in the model. As suggested by O′Donoghue et al. (*53*), the cross peaks, consistent with d_{NN}, $d_{NN}(i,i+2)$, $d_{\alpha N}(i,i+3)$, and $d_{\alpha\beta}(i,i+3)$ interactions, were all interpreted as coming from intrachain dipolar connectivities. NOE cross peaks consistent with α-helical intrachain $d_{\alpha N}(i,i+4)$ interactions were also observed. Most of the other observed cross peaks were also consistent with intrachain interactions, but approximately 100 cross peaks were clearly inconsistent with intrachain distances in the α-helical backbone structure and were therefore initially interpreted as arising from interchain interactions.

The NOESY cross peaks attributed to the interchain interactions fell into several broad categories. The γ and δ protons of the side chains of the residues in *d* positions of

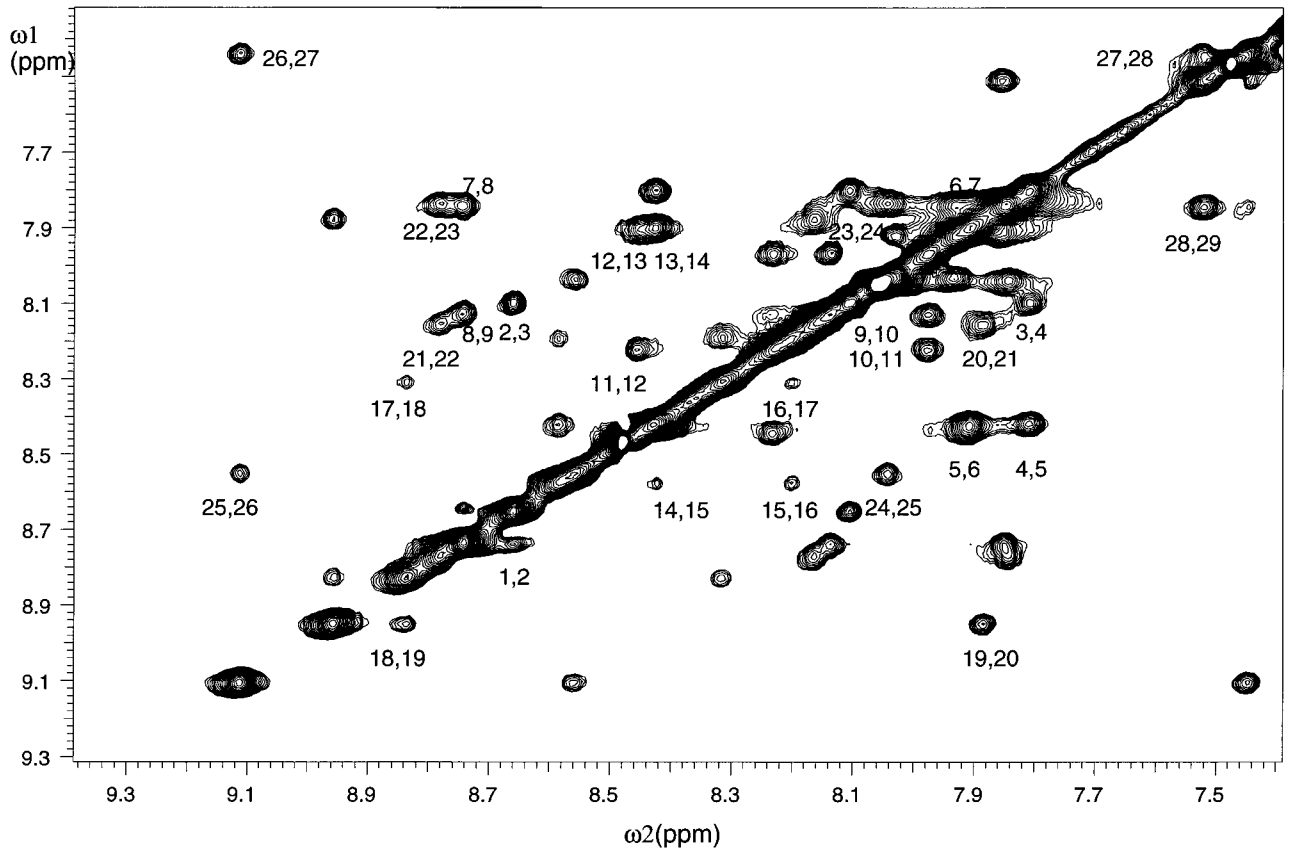

FIGURE 4: The H^N-H^N backbone region of the 150-ms NOESY spectrum of TMZip. For clarity only the highest contour levels are displayed.

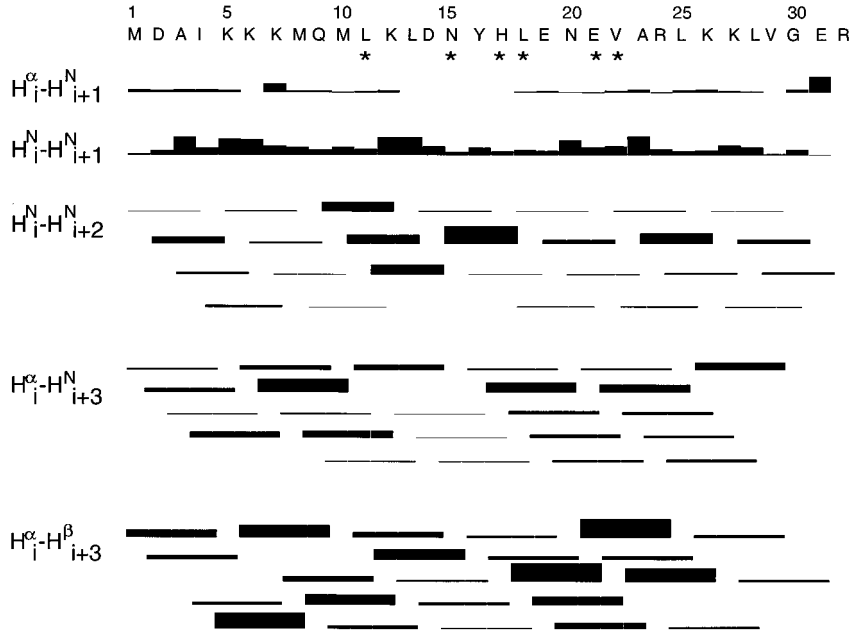

FIGURE 5: A summary of the principal NOE cross peaks used to determine the sequential assignments and secondary structure of TMZip. Residues with $^3J(H^N\text{-}H^{\alpha})$ coupling constants < 5 Hz are denoted by stars.

the heptad repeat interacted with the protons of the side chains of the residues in the following *e* and *a* positions of the opposite chain. The protons of the side chains of the residues in *g* positions interacted with the protons of the side chains of the following *a* residues of the opposite chain. Finally, the γ and δ protons of the residues in *a* positions interacted with the γ and δ protons of the residues in the following *d* positions of the opposite chain.

The assignments of the otherwise ambiguous NOESY cross peaks were carried out reiteratively with the structural refinement. For some NOESY cross peaks, potential assignments could not be distinguished because interchain and intrachain calculated distances differed by less than 0.5 Å. These distances were almost all greater than 4.5 Å and arose from connections to H^{α}, H^{β}, and H^N of residues at *a* and *d* positions in the heptad repeat. The 25 weak NOE cross

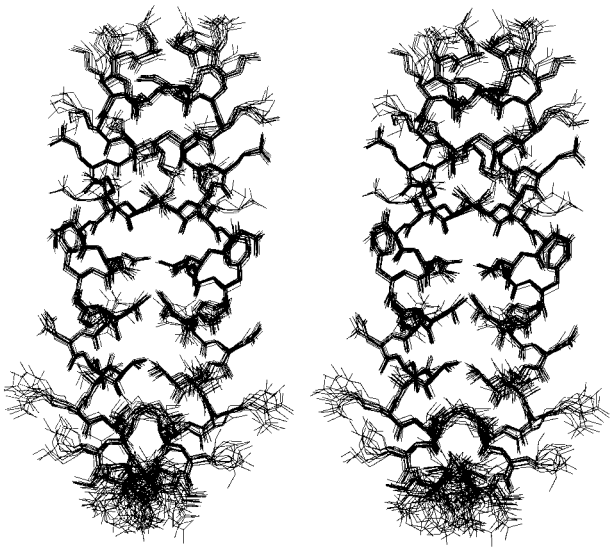

FIGURE 6: An overlay of the best 15 structures of TMZip calculated from a 50-ms NOESY spectrum using the program DIANA (*38*, *39*). The molecule is oriented with the N terminus at the top of the figure.

peaks assigned to these interactions were not used in the structural calculations. In addition, 101 strong NOE cross peaks were not used because they could not be uniquely assigned due to overlaps.

In the first cycle of structural calculations, only the upper-bound distance constraints initially assigned to intrachain interactions were included, and a family of structures for a single chain was calculated using DIANA (*38*,*39*). All the initial constraints that consistently exhibited upper-bound or significant van der Waals distance violations were removed from the data set used to define the single chain. The resulting family of structures were α-helical from residues 1−29 and showed a curvature similar to that of the Jun LZ peptide (*49*).

After the structure of a single chain was optimized, the upper-bound constraints assigned as interchain distances were added, and the structure of the two-chain species was calculated. Several NOE cross peaks, between Met-1 and Ile-4, which were originally assigned to interchain interactions on the basis of the homology model, resulted in very high target functions and consistent upper limit and van der Waals distance constraint violations in the calculated structures. If these cross peaks were attributed to intrachain interactions, however, they gave no violations in the calculated structures, and therefore the distances calculated from these NOE cross peaks were reassigned as intrachain distance constraints and the structures were recalculated. Figure 6 shows an overlay of the 15 solutions of the structure of TMZip giving the fewest constraint violations, and the corresponding structural statistics are given in Table 3.

TMZip is a two-stranded α-helical coiled coil along its entire length except for the last three C-terminal residues, but the N-terminus is somewhat less tightly packed than the C-terminus. The positions of the atoms of the first two and last two residues are poorly defined, compared with the rest of the structure. The rmsds of the heavy atoms of the side chains of residues 3−29 depended on their positions in the heptad repeat of the coiled coil: those of the side chains of *a* and *d* residues were 0.45 and 0.42 Å, respectively, while

Table 3: Summary of Distance Geometry Measurements of TMZip

Summary of Experimental Constraints

number of NOE-derived upper-limit distance constraints per molecule (two chains):	
intrachain	
intraresidue [I = j]	254
sequential [(I−j) = 1]	382
medium range [1 < (I − j) ≤ 5]	628
interchain	170
Dihedral-angle constraints per molecule	12

Maximal Constraint Violations in the 15 Best Structures

		total > 0.2 Å	interchain > 0.2 Å
maximal upper limit constraint violation	0.3 Å	13	5
maximal van der Waals constraint violation	0.3 Å	15	3
maximal dihedral-angle constraint violation	3.3°		

rmsds of Atomic Coordinates of Dimer Residues 1−32

all backbone atoms	0.56 ± 0.12 A
all heavy atoms	1.35 ± 0.23 A

rmsds of Atomic Coordinates of the Peptide Ends

residue	backbone	side chain heavy atoms
1	0.46	1.05
2	0.50	1.13
31	0.40	1.96
32	1.13	3.25

Average rmsds of the Atomic Coordinates of the Residues 3−30 in Each Position of the Heptad Repeat

position	backbone	side chain heavy atoms
a	0.26	0.45
b	0.38	0.60
c	0.34	0.85
d	0.28	0.42
e	0.27	1.30
f	0.28	0.82
g	0.28	0.89

those in the *b*, *c*, *e*, *f* and *g* positions were less well defined with values ranging from 0.6 Å to 1.3 Å. The backbone atoms, however, were well-defined for all of the positions in the heptad repeat, and the average rmsd values ranged from 0.26 Å to 0.38 Å. Unfortunately, the conformation of the N-terminal acetyl group could not be defined from the two-dimensional NMR studies because the resonances arising from the acetyl group and the epsilon methyl groups of Met 1, 8, and 10 overlapped with one another.

Differences between the NMR and Homology Modeled Structures. The structure derived from homology modeling agreed with that determined by NMR, except for the region around Asn-15. TMZip was designed with an Asn residue in an interface *a* position near the middle of the chain (residue 15), as found in natural leucine zippers including GCN4 and the Jun LZ homodimer. TMZip has an Asp in a *g* position at residue 14 while the parent GCN4 molecule has a Lys residue in the corresponding position. In the family of the 15 best NMR conformers, the HD22 atom from the side chain of each Asn-15 residue forms a hydrogen bond with either OD21 or OD22 from the Asp-14 of the opposite chain, while the HD21 atoms from each chain form weak hydrogen bonds with the O atom of Leu-11 in the same chain. The positions of the Asn-15 side chains are well-defined in solution in TMZip because one Asn-15 side chain amide proton from each chain can form a unique hydrogen bond with an acceptor from the opposite strand. In the X-ray crystal structure of GCN4 (*42*), however, the region around

Table 4: NH Deuterium Exchange and Exposed Residue Volume in TMZip

residue	position in heptad repeat	rate of deuterium exchange, $T_{1/2}$ (min) at 12.5 °C, pH 5.8[a]	protection factor	exposed volume (%)
M1	*a*	n.o.		38
D2	*b*	n.o.		47
A3	*c*	n.o.		34
I4	*d*	3.5	35	15
K5	*e*	9.9	221	33
K6	*f*	n.o.		40
K7	*g*	n.o.		24
M8	*a*	8.1	222	16
Q9	*b*	8.7	250	34
M10	*c*	ol		42
L11	*d*	11.4	120	11
K12	*e*	12.3	79	23
L13	*f*	n.o.		43
D14	*g*	9.5	361	23
N15	*a*	17.0	354	10
Y16	*b*	ol		40
H17	*c*	n.o.		30
L18	*d*	8.6	31	3
E19	*e*	10.8	440	35
N20	*f*	n.o.		33
E21	*g*	ol		16
V22	*a*	34.8	469	5
A23	*b*	13.9	311	24
R24	*c*	7.7	63	50
L25	*d*	15.8	165	5
K26	*e*	12.8	287	28
K27	*f*	ol		48
L28	*g*	14.9	34	41
V29	*a*	18.0	452	17
G30	*b*	n.o.		25
E31	*c*	ol		39
*R*32	*d*	ol		79
N15 HD21		13.1		
N15 HD22		8.4		

[a] ol, diagonal peak overlapped, no unique slowly exchanging cross peaks observed; n.o., not observed in first spectrum collected after dissolving in ^2H_2O.

the Asn residue is asymmetric with one of the Asn side chain amides on one chain acting as a hydrogen donor and one of the Asn side chain amides from the other chain acting as an H-bond acceptor. The asymmetric interchain Asn−Asn hydrogen bond is preserved in the homology modeled structure of TMZip but is not apparent in the NMR structure. The interface Asn side chain γ NH_2 proton resonances of the Jun LZ zipper show exchange broadening at low temperatures (*54, 55*). Junius et al. (*54*) suggest that, in the natural leucine zippers, one Asn amide in the *a* position acts alternatively as the hydrogen donor or acceptor, resulting in motional averaging. In contrast to TMZip, the side chains of the interface Asn in the Jun-LZ homodimer are significantly less well defined than the other residues in the *a* positions (*54, 55*).

Hydrogen Exchange. To provide further support for the coiled-coil, α-helical structure of TMZip, the rates of hydrogen exchange of backbone NH protons were measured (Table 4). As in the case of other coiled-coil peptides (*52, 54*), the rates depended both on the position of the amino acid residue in the heptad repeat of the coiled coil and on the distance from the ends of the molecule. Within a given heptad, the residues at *a, b, d,* and *e* positions showed stronger protection than those in *c* and *f* positions, a pattern consistent with being part of an α-helical coiled coil. The NH protons from the N-terminus of TMZip, the TM sequence, showed less protection than those from the GCN4 C-terminus. The protection of the residues in the N-terminus, nonetheless, still displayed a pattern consistent with their being part of an α-helical coiled coil.

Both protons of the side-chain amide NH_2 group of the Asn-15 residues were also protected from rapid exchange, suggesting they are shielded from the solvent, and probably are involved in the hydrogen bonding that is observed in the NMR structures. In contrast, the other side-chain amide protons, from Gln-9 and Asn-20, in *b* and *f* positions respectively, rapidly exchanged with deuterium, indicating that they are accessible to the solvent, as in the NMR structures.

The percent of the volume of each residue in TMZip that is solvent accessible in the average of the 15 best NMR structures is also shown in Table 4. As would be expected for a coiled coil, except for the N-terminal methionine, the residues in *a* and *d* positions are quite buried, while those in *c* and *f* positions are relatively exposed.

DISCUSSION

TMZip Structure. The structure of the N-terminus of α-tropomyosin was solved by high-resolution 2D NMR using a model peptide, TMZip, in which the first 14 residues are the N-terminus of rabbit striated α-tropomyosin and the C-terminal 18 residues are of the GCN4-P1 peptide (*43*). TMZip is a two-chained, α-helical coiled coil along the entire length, except for the last three C-terminal residues.

This is the first atomic-level structure of any region of tropomyosin, and it provides new information about this highly conserved, functionally important region of the molecule. Although McLachlan and Stewart (*6*) modeled the N-terminus as a coiled coil in their original analysis of the sequence, the ends of tropomyosin are unresolved in the 15- and 9-Å X-ray structures (*9, 10*). In these structures, tropomyosin is a coiled coil along its entire length, except for the N- and C-terminal overlap regions (the first and last nine residues). It was suggested that the ends of the tropomyosin molecule form a globular compact domain, and that neither end is highly helical (9). Our results clearly show that the N-terminal 14 residues of tropomyosin form an α-helical coiled coil in the TMZip peptide.

Although the N-terminus of TMZip may have a different structure than that of the same residues in full-length α-TM, CD analysis of other tropomyosin peptides suggests that this is not the case. Optical rotatory dispersion and CD measurements suggest that α-TM is a 100% well-defined two-chain parallel α-helical coiled coil (*7, 56*), but the N-terminal 14 residues comprise only five percent of the molecule. However, a shorter 80-residue N-terminal fragment of α-TM, where the N-terminal 14 residues are a significant fraction of the overall mass, is also 100% α-helical coiled coil based on CD analysis (Greenfield and Hitchcock-DeGregori, unpublished results). A CD study of a 32-residue model peptide of the N-terminus of α-TM also suggests that the N-terminus is part of the coiled-coil domain (*57*).

Evaluation of the Structure. The NOE data show that TMZip forms a coiled-coil α-helix from residue 1−29. All fourteen residues comprising the tropomyosin N-terminal domain of TMZip show the H^N_i-H^N_{i+1} and H^N_i-H^N_{i+2}, H^α_i-

H^{N}_{i+3}, and H^{α}_{i}-H^{β}_{i+3} NOE cross peaks characteristic of α-helices. The coiled-coil domain extends to the N-terminus, since the side chains of Met-1 from each chain pack against one another when the structure is viewed in a space-filling mode. The NH protons in *a*, *d*, *b*, and *e* positions, from residues 5−14, moreover, are protected from exchange with ^2H_2O, suggesting that they are in a coiled-coil conformation. The N-terminus, however, appears to be less tightly packed than the GCN4 half of the molecule. Met-1 and Asp-2 are poorly defined relative to the rest of the coiled-coil domain, and their rmsds are high. In addition, the hydrogen exchange protection factors of the *a* and *d* residues of residues 5−14 are approximately half that of the protection factors observed for the equivalent positions in the GCN4 half of the molecule, residues 15−29.

Because the TMZip is a parallel, symmetric, two-chained molecule, it was necessary to use a model for initial assignment of the cross peaks in the NOESY spectrum to discriminate between inter- and intrachain interactions. When the model was tested by deliberately misassigning resonances attributed to interchain interactions in the GCN4 half of TMZip as intrachain interactions, the resulting structures were of poor quality and exhibited many significant constraint violations. The same held true when most of the resonances in the tropomyosin half were deliberately misassigned. However, in the tropomyosin half, several initial assignments based on the model were reassigned because the original attributions gave consistent van der Waals or upper limit constraint violations when the NMR structure was calculated.

Implications of the Structure. Our determination of the coiled-coil structure of α-TM gives insight into the function of this highly conserved region of TM. Mutation of the residue corresponding to Met-8 of TMZip in the tropomyosin TPM3 results in nemaline myopathy, a disease of skeletal muscle (*19*). Since Met-8 is in an *a* position at the coiled-coil interface, the mutation would greatly destabilize the coiled-coil structure of the N-terminus. When Met-8 was mutated to Arg in full-length rat recombinant α-TM expressed in *Escherichia coli*, the mutation decreased the T_M of folding by 1.5 °C (Greenfield and Hitchcock-DeGregori, unpublished results) and it decreased the affinity of the mutant protein for actin more than 100-fold (Hitchcock-DeGregori and Liu, unpublished results).

The NMR structure of TMZip also provides information about residues which may be involved in interactions involving the N-terminus of tropomyosin. The charged residues, Asp-2, Lys-5, and Lys-6, are highly exposed at *b*, *e*, and *f* positions of the heptad repeat in TMZip (Table 4). Lys-7 is only 24% exposed to the solvent in a *g* position (Table 4), but the charged amino end is on the surface. Lys-5, -6, and -7 are among the most highly reactive of all the lysines of α-TM to modification with acetic anhydride, consistent with their being exposed to solvent (*58*). These residues could provide charged surfaces for polymerizing interactions with residues at the C-terminus of tropomyosin, as suggested by McLachlan and Stewart (*6*). Acetylation of Lys-7 results in loss of tropomyosin polymerizability (*59*), suggesting that it is indeed involved in the end-to-end interactions of tropomyosin. In addition, the hydrophobic residues, Met-10 and Leu-13, are both greater than 40% exposed in TMZip. They are in successive *c* and *f* positions on the same side of each α-helix in the coiled coil and form a hydrophobic face which would be available for binding interactions.

ACKNOWLEDGMENTS

We would like to thank Dr. Gerald D. Fasman for providing the convex constraint algorithm program. We would also like to thank G. V. T. Swapna, Chen-ya Chien, and Carlos Rios for their help with the acquisition and processing of the NMR data.

SUPPORTING INFORMATION AVAILABLE

A table listing the chemical shifts of the protons of TMZip (2 pages). Ordering information is given on any current masthead page.

REFERENCES

1. Lees-Miller, J. P., and Helfman, D. M. (1991) *Bioessays 13*, 429−437.
2. Lehrer, S. S. (1994) *J. Muscle Res. Cell Motil. 15*, 232−236.
3. Tobacman, L. S. (1996) *Annu. Rev. Physiol. 58*, 447−481.
4. Hitchcock-DeGregori, S. E. (1994) in *Actin: Biophysics, Biochemistry and Cell Biology* (Estes, J. E., and Higgins, P. J., Eds.) pp 85−96, Plenum Press, New York.
5. Hammell, R. E., and Hitchcock-DeGregori, S. E. (1996) *J. Biol. Chem. 271*, 4236−4242.
6. McLachlan, A. D., and Stewart, M. (1975) *J. Mol. Biol. 98*, 293−304.
7. Lehrer, S. S. (1975) *Proc. Natl. Acad. Sci. U.S.A. 72*, 3377−3381.
8. Stewart, M. (1975) *FEBS Lett. 53*, 5−7.
9. Phillips, G. N., Jr., Fillers, J. P., and Cohen, C. (1986) *J. Mol. Biol. 192*, 111−131.
10. Whitby, F. G., Kent, H., Stewart, F., Stewart, M., Xie, X., Hatch, V., Cohen, C., And Phillips, G. N., Jr. (1992) *J. Mol. Biol. 227*, 441−452.
11. O'Brien, E. J., Bennett, P. M., and Hanson, J. (1971) *Philos. Trans. R. Soc. London, Sec. B 261*, 201−208.
12. Milligan, R. A., Whittaker, M., and Safer, D. (1990) *Nature 348*, 217−221.
13. Karlik, C. C., and Fyrberg, E. A. (1986) *Mol. Cell. Biol. 6*, 1985−1993.
14. Hitchcock-DeGregori, S. E., and Heald, R. W. (1987) *J. Biol. Chem. 262*, 9730−9735.
15. Heald, R. W., and Hitchcock-DeGregori, S. E. (1988) *J. Biol. Chem. 263*, 5254−5259.
16. Cho, Y. J., and Hitchcock-DeGregori, S. E. (1991) *Proc. Natl. Acad. Sci. U.S.A. 88*, 10153−10157.
17. Willasden, K. A., Butters, C. A., Hill, L. E., and Tobacman, L. S. (1992) *J. Biol. Chem. 267*, 23746−23752.
18. Cho, Y. J., Liu, J., and Hitchcock-DeGregori, S. E. (1990) *J. Biol. Chem. 265*, 538−545.
19. Laing, N. G., Wilton, S. D., Akkari, P. A., Dorosz, S., Boundy, K., Kneebone, C., Blumbergs, P., White, S., Watkins, H., Love, D. R., and Haan, E. (1995) *Nat. Genet. 9*, 75−79.
20. Stone, D., Sodek, J., Johnson, P., and Smillie, L. B. (1975) *Proc. FEBS Meet. (Budapest) 31*, 125−136.
21. Stone, D., and Smillie, L. B. (1978) *J. Biol. Chem. 253*, 1137−1148.
22. Landschultz, W. H., Johnson, P. F., and McKnight, S. L. (1988) *Science 240*, 1759−1764.
23. Greenfield, N. J., and Hitchcock-DeGregori, S. E. (1993) *Protein Sci. 2*, 1263−1273.
24. Edelhoch, H. (1967) *Biochemistry 6*, 1948−1954.
25. Gill, S. C., and von Hipple, P. H. (1989) *Anal. Biochem. 182*, 319−326.
26. Fasman, G. D. (1989) *Practical Handbook of Biochemistry and Molecular Biology*, CRC Press, Baton Raton.
27. Eftink, M. R., Ionescu, R., Ramsay, G., Wong, C.-Y., and Maki, A. H. (1996) *Biochemistry 35*, 8084−8094.

28. Hoshino, M., Yumoto, N., Shikawa, S. Y., and Goto, Y. (1997) *Protein Sci. 6*, 1396−1404.
29. Perczel, A., Hollósi, M., Tusnády, G., and Fasman, G. D. (1991) *Protein Eng. 4*, 669−679.
30. Perczel, A., Park, K., and Fasman, G. D. (1992) *Anal. Biochem. 203*, 83−93.
31. Piantini, U., Sørensen, O. W., and Ernst, R. R. (1982) *J. Am. Chem. Soc. 104*, 6800−6801.
32. Jeener, J., Meier, B. H., Bachmann, P., and Ernst, R. R. (1979) *J. Chem. Phys. 71*, 4546−4553.
33. Braunschweiler, L., and Ernst, R. R. (1983) *J. Magn. Reson. 54*, 521−528.
34. Marion, D., and Wüthrich, K. (1983) *Biochem. Biophys. Res. Commun. 113*, 967−974.
35. States, D. J., Haberkorn, R. A., and Rubin, D. J. (1982) *J. Magn. Reson. 48*, 286−292.
36. Wüthrich, K. (1986) *NMR of Proteins and Nucleic Acids*, John Wiley and Sons, New York.
37. Wüthrich, K., Billeter, M., And Braun, W. (1983) *J. Mol. Biol. 169*, 949−961.
38. Braun, W., and Go, N. (1985) *J. Mol. Biol. 186*, 611−626.
39. Güntert, P., Braun, W., And Wüthrich, K. (1991) *J. Mol. Biol. 217*, 517−530.
40. Koradi, R., Billeter, M., and Wüthrich, K. J. (1996) *J. Mol. Graphics 14*, 51−55.
41. Bai, Y., Milne, J. S., Mayne, L., and Englander, S. W. (1993) *Proteins: Struct., Funct., Genet. 17*, 75−86.
42. O'Shea, E. K., Klemm, J. D., Kim, P. S., and Alber, T. (1991) *Science 254*, 646−648.
43. Oas, T. G., McIntosh, L. P., O'Shea, E. K., Dahlquist, F. W., and Kim, P. S. (1990) *Biochemistry 29*, 2891−2894.
44. Olive, M., Williams, S. C., Dezan, C., Johnson, P. F., and Vinson, C. (1996) *J. Biol. Chem. 271*, 2040−2047.
45. Trybus, K. M., Freyzon, Y., Faust, L. Z., and Sweeney, H. L. (1997) *Proc. Natl. Acad. Sci. U.S.A. 94*, 48−52.
46. Hitchcock-DeGregori, S. E., and An, Y. (1996) *J. Biol. Chem. 271*, 3600−3603.
47. Hammell, R. E., and Hitchcock-DeGregori, S. E. (1997) *J. Biol. Chem.272*, 22409−22416.
48. Thompson, K. S., Vinson, C. R., and Freire, E. (1993) *Biochemistry 32*, 5491−5496.
49. Junius, F. K., Weiss, A. S., and King, G. F. (1993) *Eur. J. Biochem. 214*, 415−424.
50. Saudek, V., Pastore, A., Castiglione Morelli, M. A., Frank, R., Gausepohl, H., Gibson, T., Weih, F., and Roesch, P. (1990) *Protein Eng. 4*, 3−10.
51. Wishart, D. S., Sykes, B. D., and Richards, F. M. (1992) *Biochemistry 31*, 1647−1651.
52. Goodman, E. M., and Kim, P. S. (1991) *Biochemistry 30*, 11615−11620.
53. O'Donoghue, S. I., Junius, F. K., and King, G. F. (1993) *Protein Eng. 6*, 557−564.
54. Junius, F. K., Mackay, J. P., Bubb, W. A., Jensen, S. A., Weiss, A. S., and King, G. F (1995) *Biochemistry 34*, 6164−6174.
55. Junius, F. K., O'Donoghue, S. L., Nilges, M., Weiss, A. S., and King, G. F. (1996) *J. Biol. Chem. 271*, 13663−13667.
56. Cohen, C., and Szent-Györgyi, A. G. (1957) *J. Am. Chem. Soc. 79*, 248.
57. Greenfield, N. J., Stafford, W. F., and Hitchcock-DeGregori, S. E. (1994) *Protein Sci. 3*, 402−410.
58. Hitchcock-DeGregori, S. E., Lewis, S. F., and Chou, T. M.-T. (1985) *Biochemistry 24*, 3305−3314.
59. Johnson, P., and Smillie, L. B. (1977) *Biochemistry 16*, 2264−2269.

BI973167M